Stone-based Smart Aggregates using PZT for Compressive Seismic Stress Monitoring

S.Hou, H.B. Zhang& J.P. Ou
Dalian University of Technology, Dalian

J.P. Ou
Harbin Institute of Technology, Harbin

SUMMARY:
A stone-based smart aggregate using PZT (Lead Zirconate Titanate), as the sensing element for compressive seismic stress monitoring is developed. The smart aggregate consists of a piece of PZT patch sandwiched between a pair of marble blocks through epoxy. With a commercially-available charge amplifier, the frequency response of both the amplitude and the phase shift of the sensing system are investigated by applying the frequency sweep loading scheme on the proposed smart aggregate. The servo-hydraulic machine was used for applying the alternating load. Investigation on the deterioration process of the piezoelectric coefficient of the selected PZT material was conducted. The findings show that for the selected PZT material, the degradation of the piezoelectric coefficient is negligible under the pre-stress considered; with a commercially-available charge amplifier, the smart aggregate can monitor the seismic response of low and middle-rise building structures under moderate earthquakes.

Keywords: Smart aggregates; PZT; compressive stress; degradation

1. INSTRUCTION

One of the major obstacles in the research of seismic collapse mechanisms for concrete building structures is the lack of a reliable method to monitor its internal stress during the collapse stage. Traditional strain gauges, like FBG sensors and foil strain gauges, when embedded in a structure could give stress information by using the material constitutive law. However, there exists great uncertainty during the nonlinear stage, and its bondage with concrete is questionable during the cyclic loading. A commercially-available load cell is able to measure the internal stress directly. However, issues such as the size, the bondage with concrete, the interference to the local stress field, and the cost may hinder its application.

Based on the evaluation of the stress wave propogation in concrete, a cement-based smart aggregate was proposed by Song *et al.*(2005) for damage identification in concrete structures. It was also used in early concrete strength monitoring (Gu *et al.*, 2006), over height vehicle-bridge collision monitoring (Song *et al.*, 2007), and structural health monitoring of other concrete structures (Yan *et al.*, 2009; Gu *et al.*, 2010; Laskar *et al.*, 2009; Moslehy *et al.*, 2010). This monitoring method is able to qualitatively evaluate the structure state, while the stress history of the structure cannot be obtained during the damage process. Utilizing the direct piezoelectric effect, the smart aggregate is used in traffic load measurement on the road (Yang *et al.*, 2005; Li *et al.*, 2006). PZTs and PVDFs in the form of patches were utilized for low strain measurement (Jayant and Inderjit, 2000). However, so far their application in relatively high stress/strain is unfound.

In the sensor application for PZT material for stress measurement, the piezoelectric response is linear and reversible when subjected to a small stress (IEEE, 1988). However, under relatively high stress, the irreversible changes in the material, which takes a finite time, will cause hysteresis. For a soft PZT (P-5H), it is found that its piezoelectric coefficient varies with both the level of the static pre-stress and the dynamic stress amplitude (Alguero *et al.*, 2001). For a selected PZT material, the piezoelectric coefficient drops by 50% when subjected to pre-stress of 30 MPa and increases by 11% per MPa stress. The significant degradation in the piezoelectric coefficient for the soft PZT when subjected to pre-stress was also found by other researchers (Yimnirun *et al.*, 2006; Yang *et al.*, 2001; Calderon-Moreno, 2001).

The dependence of the piezoelectric property of PZT on the static pre-stress and the dynamic stress amplitude will restrict its application in seismic stress measurement. In this paper, a marble-based smart aggregate sensor using PZT material for seismic compressive stress monitoring is developed. Its application in monitoring the relatively high stress is evaluated via experiments. The loading scheme of alternating stresses superimposing on static pre-stress was performed through a servo-hydraulic machine for its calibration.

2. SENSING PRINCIPLE

Under small field conditions, the constitutive relations for a piezoelectric material are (IEEE, 1988)

$$D_i = e_{ij}^{\sigma} E_j + d_{im}^{d} \sigma_m \tag{2.1}$$

$$\varepsilon_k = d_{jk}^{c} E_j + s_{km}^{E} \sigma_m \tag{2.2}$$

which can be rewritten as

$$\begin{bmatrix} D \\ \varepsilon \end{bmatrix} = \begin{Bmatrix} e^{\sigma} & d^{d} \\ d^{c} & s^{E} \end{Bmatrix} \begin{bmatrix} E \\ \sigma \end{bmatrix} \tag{2.3}$$

where a vector D of size (3×1) is the electric displacement (Coulomb/m^2), ε is the strain vector (6×1), E is the applied electric field vector (3×1) (Volt/m), and σ_m is the stress vector (6×1) (N/m2). The piezoelectric constants are the dielectric permittivity e_{ij}^{σ} of size (3×3) (Farad/m), the piezoelectric coefficients d_{im}^{d} (3×6) and d_{jk}^{c} (6×3) (Coulomb/N or m/Volt), and the elastic compliance s_{km}^{E} of size (6×6) (m2/N). For a patch of piezoelectric material (see Fig. 2.1), the poling direction, which is usually along the thickness, is denoted as the 3-axis. The 1-axis and 2-axis are in the plane of the patch. In the case of a stress sensor, where the applied external electric field is zero, Eqn. 2.3 becomes

$$\begin{bmatrix} D_1 \\ D_2 \\ D_3 \end{bmatrix} = \begin{bmatrix} 0 & 0 & 0 & 0 & d_{15} & 0 \\ 0 & 0 & 0 & d_{24} & 0 & 0 \\ d_{31} & d_{32} & d_{33} & 0 & 0 & 0 \end{bmatrix} \begin{Bmatrix} \sigma_1 \\ \sigma_2 \\ \sigma_3 \\ \sigma_4 \\ \sigma_5 \\ \sigma_6 \end{Bmatrix} \tag{2.4}$$

where σ_1, σ_2, and σ_3 are the normal stress in the 1, 2, and 3 direction respectively, σ_4, σ_5, and σ_6 are the shear stresses in the 2-3, 1-3, and 2-3 planes respectively, and the coefficients d_{31}, d_{32}, and d_{33} relate the normal stress in the 1, 2, and 3 directions respectively to a field along the poling direction, D_3. The coefficients d_{15} and d_{24} relate the shear stress in the 1-3 plane to the field D_1 and the shear stress in the 2-3 plane to the field D_2.
The electric displacement can be related to the generated charge with relation to

$$q = \iint \begin{bmatrix} D_1 & D_2 & D_3 \end{bmatrix} \begin{Bmatrix} dA_1 \\ dA_2 \\ dA_3 \end{Bmatrix} \tag{2.5}$$

where dA_1, dA_2, and dA_3 are the components of the electrode area in the 2-3, 1-3, and 1-2 planes respectively. When the PZT is used to measure the uniaxial compressive stress, it is generally in the thin form of patches with its two faces coated with thin electrode layers with the applied stress in the 3 direction. Since the areas of A_1 and A_2 is much smaller than that of A_3, Eqn. 2.5 can be rewritten as

$$q = D_3 A_3 \tag{2.6}$$

Substituting Eqn. 2.4 into Eqn. 2.6 gives

$$q = \sum_{i=1}^{3} d_{3i} \sigma_i A_3 \tag{2.7}$$

The charge q can be converted to the voltage V by charge-voltage converter in the relation

$$V = \frac{q}{C} \tag{2.8}$$

where C is the capacitance of the feedback capacitor of the converter.

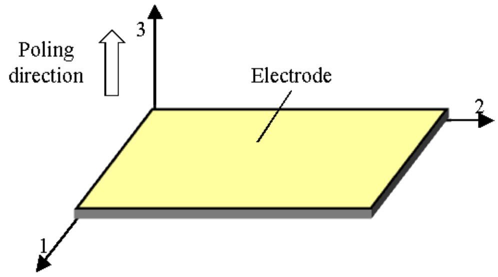

Figure 1.1. PZT patch and poling direction

3. DESIGN AND FABRICATION OF THE SMART AGGREGATE

The proposed smart aggregate is expected both to survive the concrete crushing state and to have good compatibility with the concrete. Fig. 3.1 demonstrates its structure. The proposed smart aggregate consists of a piece of PZT patch connected with a piece of two-wire cable and a pair of marble blocks. The commercially-available soft PZT ceramic referred to as P-5H with a major composition of $Pb(TiZr)O_3$ which features high sensitivity was chosen. The PZT's properties, measured by the supplier, are listed in Table 3.1. Although the hard PZT is reportedly more resistant to degradation in the piezoelectric coefficient when it is under pre-stress (Yimnirun et al., 2006; Yang et al., 2001; Calderon-Moreno, 2001), the proposed smart aggregate is also designed to function as an actuator thus a pair of the smart aggregates can work together to provide active sensing. As a trade-off, its degradation of the piezoelectric coefficient is required within an acceptable level in the view of practical application. The Young's modulus of the marble and the epoxy used in this paper is 51.5 GPa and 2.5 GPa respectively, as supplied by the manufacturer. The size of the PZT patch is 15 mm×15 mm, and the thickness is 0.3 mm. The PZT patch was connected to the two-wire cable on its two sides at the position close to its edge through welding. The marble was cut into a 25×25×12 mm cube. Afterward, they were aligned together along the 12 mm long side and were held tightly by a clamp. Along one central line in the interface between the two marble blocks, a hole with a diameter of 3 mm and depth of 10 mm was bored to accommodate the connected cable and the welding points on the PZT patch. Then the PZT patch was sandwiched between a pair of marble blocks though epoxy. After the epoxy was cured, the thickness of the epoxy layer is measured to be about 0.45 mm.

The compressive strength of commonly-used concrete is generally not higher than 60 MPa. At this stress level, the PZT material is in the elastic stage (Calderon-Moreno, 2001), as are the marble and the epoxy. Therefore, as a whole, the proposed marble-based smart aggregate works in the linear range. While the cement-based smart aggregate is subject to cracking in the cement at this stress level due to the existence of micro cracks after the cement is cured. Therefore, the proposed smart aggregate is more stable and reliable in comparison with the cement-based smart aggregate. Moreover, compared with the cement-based smart aggregate, the PZT patch in the smart aggregate can be easily fixed during its fabrication. This endows the proposed smart aggregate with higher accuracy for stress measurement than the cement-based smart aggregate.

The sensitivity of the proposed smart aggregate is defined as

$$S = \frac{Q}{\sigma} \tag{3.1}$$

Where σ is the compressive stress on the smart aggregate along the poling directon of the PZT patch. From Eqn. 2.7, the sensitivity can be related to the piezoelectric coefficient of the PZT patch by

$$S = \sum_{i=1}^{3} A_3 \alpha_i \, d_{3i} \tag{3.2}$$

where α_i is the stress ratio expressed as

$$\alpha_{3i} = \frac{\sigma_i}{\sigma}, \quad i = 1,2,3 \tag{3.3}$$

The sensitivity can also be defined as the smart aggregate output voltage vs. the applied stress. For example,

$$S = \frac{V}{\sigma} \tag{3.4}$$

V is the generated voltage which can be obtained by Eqn. 2.8.

Table 3.1. Typical properties of the selected PZT P-5H.

Young's modulus(GPa)	46
Density(kg/m^3)	7.45
d_{31}, d_{32} (pC/N)	-186
d_{33}(pC/N)	670
d_{15}(pC/N)	660

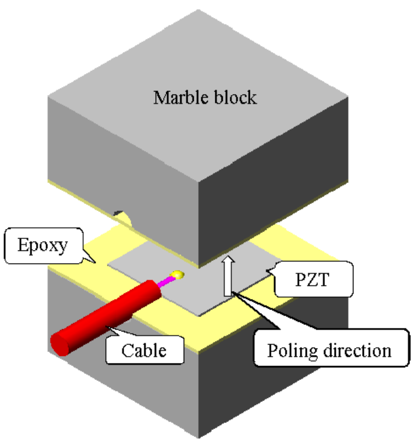

Figure 3.1. Structure of the proposed smart aggregate

The sensitivity of the developed smart aggregate has also been calculated theoretically. The finite element analysis (by ABAQUS 6.10) was carried out to calculate the stress distribution within the smart aggregate when it is subject to the uniform stress along the PZT's thickness direction. The analysis results are shown in Fig. 3.2. For the proposed smart aggregate, the 1 and 2 directions are parallel to the plane of the PZT patch. Additionally, the 1 and 2 directions are parallel and perpendicular to the direction of the hole in the marble, respectively. The 3 direction is parallel to the thickness direction of the PZT patch. The ratio of the average compressive stress in the PZT patch in the 1, 2, and 3 directions to the stress on the smart aggregate in the 3 direction are 0.324, 0.289, and 1.22, respectively. The charge generated by the stress in the 1 and 3 directions accounts for 16 percent of the total charge only, indicating that the sensor is not sensitive to the stress in the 1 and 2 directions. For the smart aggregate, its sensitivity expressed by the generated charge vs. stress can be calculated from Eqn. 3.10. The calculated value is 1.58×10^5 pC/MPa. For the commonly used charge amplifier with a maximum charge input of 1.0×10^6 pC, the maximum stress that the smart aggregate can measure is 6.3 MPa, corresponding to the only moderate seismic response of building structures. To monitor the stage of concrete crushing, the amplitude range of stress of the sensing system should be extended by using the charge-to-voltage converter with a larger maximum input charge.

During the fabrication of the smart aggregate, it is difficult to keep the thickness of the epoxy layer constant. The influence of the thickness variation to the ratio of the stress on the PZT patch to the stress on the smart aggregate (“SA” or “SA sensor”) in the 3 direction is evaluated by the finite element analysis. The thickness of the epoxy layer in the range of 0.3 - 1mm is considered. The analysis results are given in Fig. 3.3. It shows that as the epoxy layer thickness increases, the stress ratio decreases. The measured thickness of the epoxy layer varies within the range of 0.35 - 0.55 mm. In this range, the ratio of the stress in the PZT patch in the 3 direction to the stress on the smart aggregate in the 3 direction varies from 1.28 to 1.16 only. Therefore, the influence of the epoxy thickness variation on the smart aggregate sensitivity is not significant.

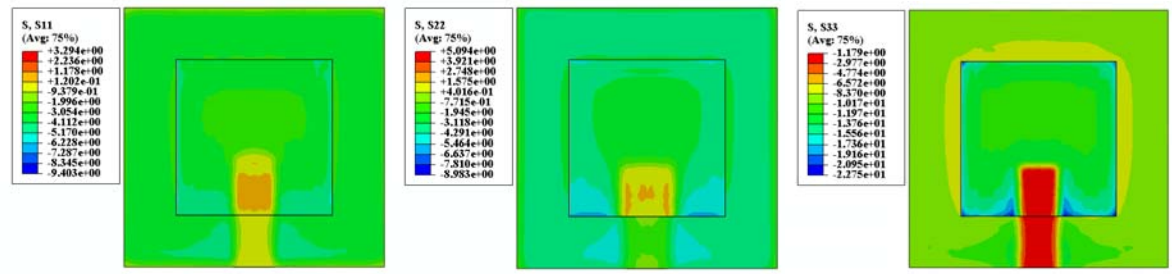

(a) (b) (c)

Figure 3.2. Stress distribution in the mid interface of the smart aggregate in the:
(a)1 direction, (b) 2 direction and (c) 3 direction.

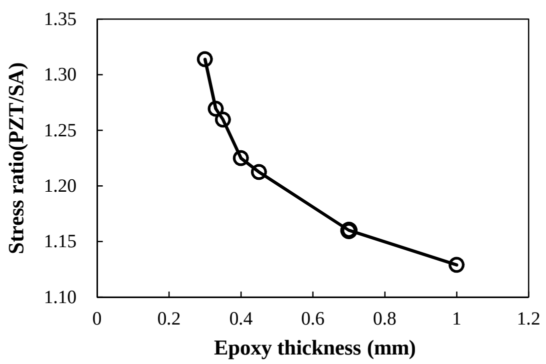

Figure 3.3. Stress ratio (PZT/SA) vs. epoxy thickness

4. EXPERIMENTAL RESULTS

4.1. Experimental Setup

The test configuration is illustrated in Fig. 4.1. The alternating stress superimposed on the compressive static stress is applied on the smart aggregate by the servo-hydraulic test machine (MTS 810). The generated charge signal will be converted to the voltage signal by a charge amplifier (HK9301, Hengke Tech. Co., China). The converted voltage signals then were measured by the data acquisition system (NI4472 module, National Instruments), which also measures the load signal applied by the servo-hydraulic test machine. Fig. 4.2 shows the picture of the test system.

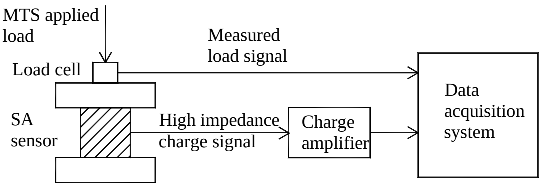

Figure 4.1. Test configuration of the test system

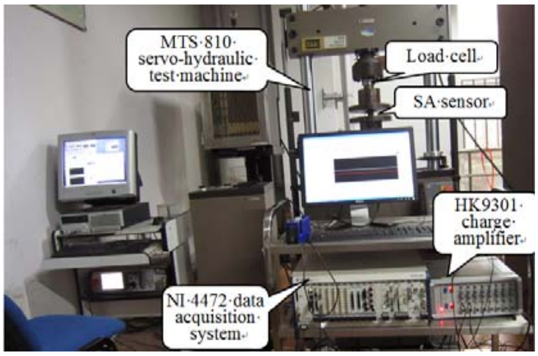

Figure 4.2. Picture of the test system

4.2. Frequency Response of the Sensing System

The frequency response of the sensing system was investigated by applying a frequency sweep loading scheme on a smart aggregate as shown in Fig. 4.3**Error! Reference source not found.**. The sine wave stress with amplitude of 2.1 MPa and frequency range of 0.05-10 Hz was applied on the smart aggregate which was also applied with a 3.2 MPa compressive pre-stress. For the smart aggregate, the frequency response of both the amplitude and the phase shift are shown in Fig. 4.4. From this figure, it can be determined that the lower bound of the frequency response for the sensing system is 0.5 Hz, above which the amplitude remains constant. In addition, the phase shift is less than 18 degrees which can cause errors of no more than five percent. This sensing system can work only for the seismic stress monitoring of low and middle-rise building structures. To monitor the seismic response of high-rise building structures, the lower bound of the frequency response of the charge-voltage converter should be reduced to a much lower value.

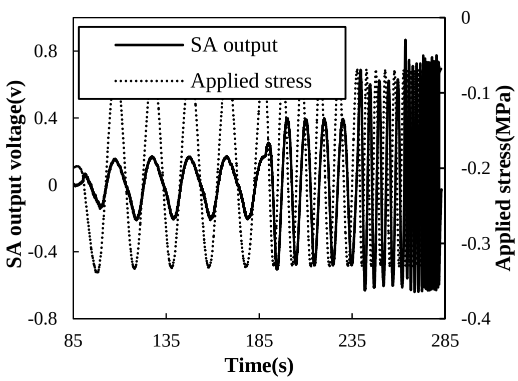

Figure 4.3. Frequency sweep loading scheme

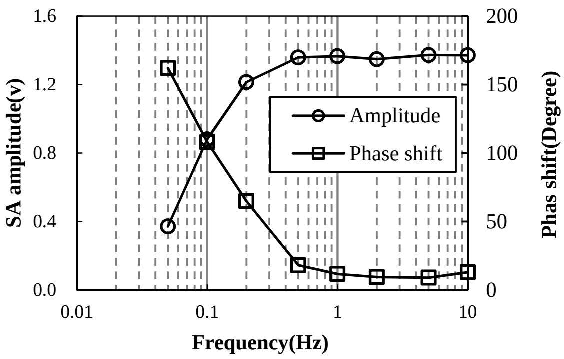

Figure 4.4. Frequency response of both amplitude and the phase shift of the smart aggregate

4.3. Depolarization Process of the PZT Under Pre-stress

When the PZT material is subjected to static loading, depolarization will occur which has time dependence. This process is a consequence of the slow movement of the ferroelastic domain wall under stress. The calibration of the proposed smart aggregate could start only after this depolarization process has finished. The time dependence of the process for the PZT used in this paper is investigated by evaluating its sensitivity variation. Measurement was performed on a pair of identical smart aggregates, denoted as SA1 and SA2, which were aligned together and were applied with two levels of pre-stresses, 4.8 MPa and 14.4 MPa respectively for 30 minutes. Meanwhile, a series of alternating stresses were superimposed on the pre-stress for measuring the sensor's sensitivity. These two level pre-stresses correspond to the low and high axial load that might occur in concrete building structures. The loading scheme is shown in Fig. 4.5. As an example, Fig. 4.6 shows the applied alternating stresses during 994 - 1006 s, which consists of a group of sine wave stresses with ever-increase amplitudes up to 2.4MPa, and frequency of 3Hz. It can be seen that the responses of these two smart aggregates are quite close. The ratio of the amplitude of the alternating stress to the amplitude of the smart aggregate output voltage was calculated as the smart aggregate sensitivity, which is shown in terms of generated voltage per unit stress as shown in Fig. 4.7. With the stress amplitude up to 2.24 MPa, the nonlinear piezoelectric response is not found as presented by Alguero *et al.*, (2001). The sensitivities of the two smart aggregates measured in this duration are 0.628 and 0.605 V/MPa respectively. The difference in the sensitivity between them is only approximately 2 percent, indicating that the fabrication technique used in this paper is proper and reliable.

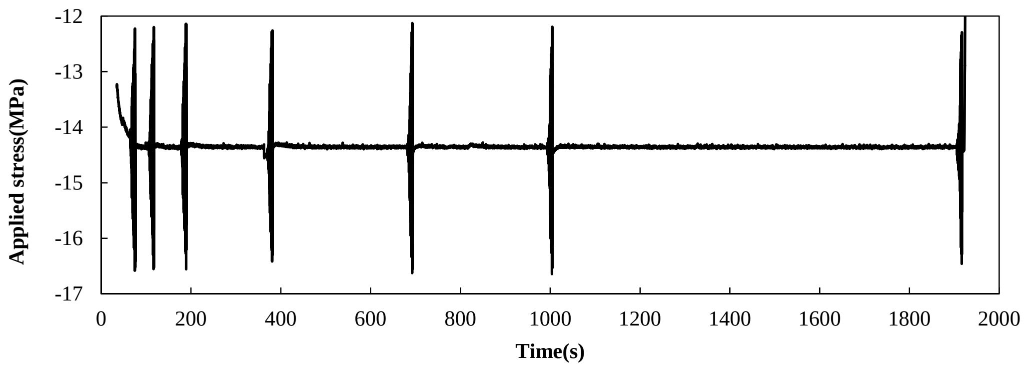

Figure 4.5. Load history

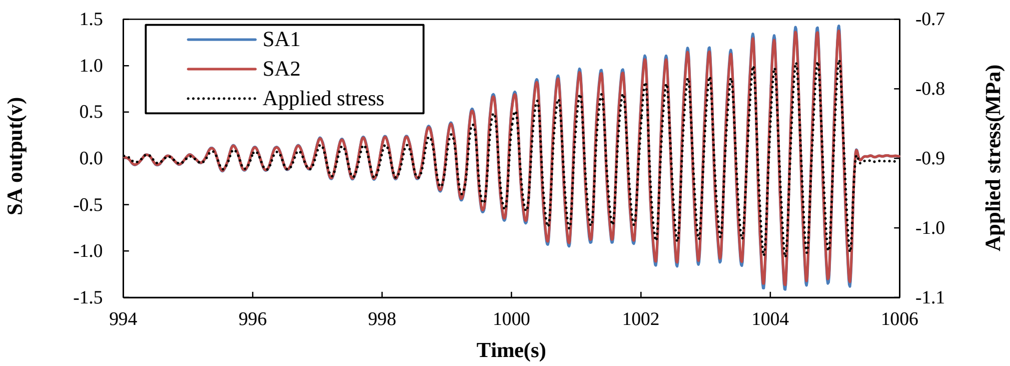

Figure 4.6. The applied sine stress waves and the smart aggregate output during 994-1006s

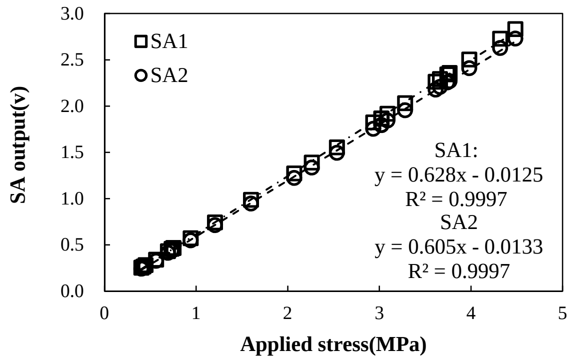

Figure 4.7. Amplitudes of smart aggregate output vs. applied stress during 994-1006s

The variations of the smart aggregate sensitivities under the two pre-stress levels are shown in Fig 4.8. Here the sensitivities of the smart aggregates were normalized to their initial values. It was found that over the duration of 30 minutes, the depolarization process was fast in the beginning and became slow afterward. At the stress level of 14.4 MPa, the depolarization completed within 15 minutes. However, at the stress level of 4.8 MPa, the depolarization seemed to take a longer time. Additionally, at the stress level of 4.8 MPa, the sensitivity dropped by 3% during the first 15 minutes and dropped 2% in the consecutive 15 minutes, showing a trend of deceleration. Thus, it can be concluded that for concrete building structures with common pre-stress, 15 minutes is the proper time for exhausting most of the depolarization process. In the following tests in this paper, 15 minutes is used as the waiting time before the calibration starts.

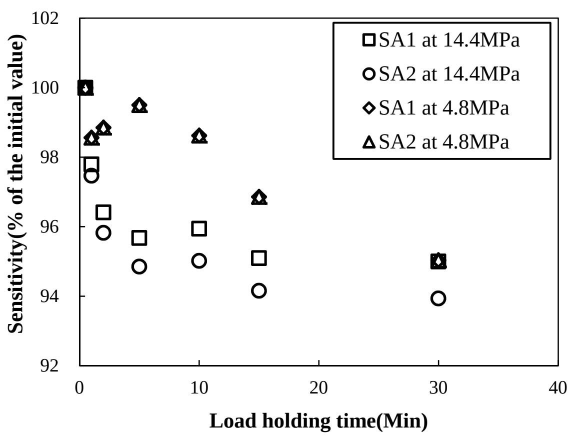

Figure 4.8. Sensitivity variation of SA vs. holding time

4.4. Influence of Pre-stress to Smart Aggregate Sensitivity

Arranged in cascades with a step of 4.8 MPa within the range 4.8 - 24 MPa, the compressive pre-stress was applied on the aligned sensors of SA1 and SA2 (see Fig. 4.9). In each step, the stresses were held for 15 minutes, and at the end, a group of ever-increasing alternating stress was superimposed on the pre-stress for evaluating the smart aggregate's sensitivity. Fig. 4.10 shows an example of the alternating stresses, which are the same as depicted previously. The variations of the smart aggregate sensitivity at each load level are drawn in Fig. 4.11. Here the sensitivities were normalized against their values measured at the load level of 4.8 MPa. It can be seen that for the smart aggregates, even at the pre-stress level of 24 MPa, their sensitivities drop no more than 3%. This means that the influence of the pre-stress on the piezoelectric coefficient in the level of interest is negligible. This finding differs greatly from the results presented by previous researchers (Alguero *et al.*, 2001; Yimnirun *et al.*, 2006; Yang *et al.*, 2001; Calderon-Moreno, 2001), indicating that for the soft PZT materials with different compositions, the extent of degradation in the piezoelectric response might be different when it is subjected to pre-stress. This finding is very appealing since the initial static load differs greatly in building structures according to locations, and it is difficult to be predetermined accurately.

Since the influence of the pre-stress on the proposed smart aggregate is negligible, the values given in Fig. 4.7 can be referred to as the sensitivities of these two smart aggregates. Their average value is 0.617 V/MPa. The capacitance of the feedback capacitor of the charge amplifier used in this paper is 200 nF. The average sensitivity of them can be converted to 1.23×10^5 pC/MPa in terms of the output charge per unit stress. This value is about 22% smaller than the analytical result of 1.58×10^5 pC/MPa. The difference may come from two factors. The first one is the uncertainty in stress distribution obtained from the finite element analysis. For example, to simplify the modeling of the smart aggregate, the material property of the cable which is connected to the PZT patch inside the hole area is assumed to be the same as the epoxy, and the welding point on the PZT patch is not considered during modeling. The second factor comes from the deterioration of the piezoelectric coefficient which could cause decreases up to 5 percent as indicated from the test results presented previously.

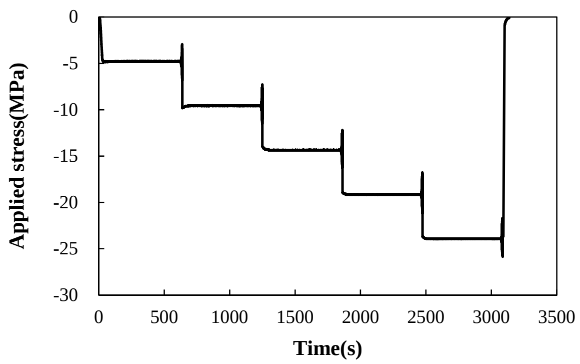

Figure 4.9. The applied stress for evaluating the influence of pre-stress

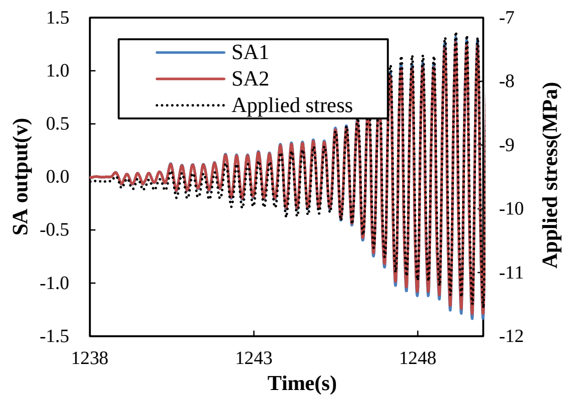

Figure 4.10. Applied sine wave stress during 1238-1250s

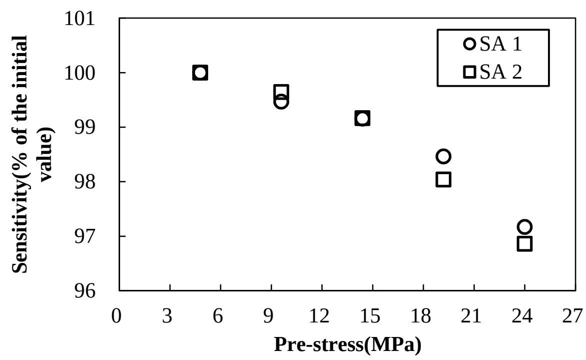

Figure 4.11. Smart aggregate sensitivity vs. pre-stress

5. DISCUSSIONS AND CONCLUSION

As reported in this paper, a marble-based smart aggregate as a seismic compressive sensor is proposed. The smart aggregate consists of a piece of PZT patch sandwiched between a pair of marble blocks through epoxy. This structure and fabrication technique renders higher stability in its mechanical performance and higher consistency in its fabrication quality in comparison with the cement-based smart aggregate. Under pre-stresses of up to 24 MPa, the smart aggregate's sensitivity drops no more than 3%. Under a dynamic load with amplitude of 2.25 MPa, nonlinearity in its piezoelectric response is not observed. With the proposed smart aggregate and a commercially-available charge amplifier, the sensing system for dynamic compressive stress has a lower bound of frequency response of 0.5 Hz and upper bound stress amplitude of 8.3 MPa, which is capable of monitoring the seismic response of low and middle-rise buildings subject to moderate earthquakes.

AKCNOWLEDGEMENT

Joint financial supports from the National Science Foundation of China (Grant no. 50908031, 51161120359) are gratefully acknowledged.

REFERENCES

Alguero M, Cheng B L, Guiu F, Reece M J, Poole M and Alford N. (2001). Degradation of the d33 piezoelectric coefficient for PZT ceramics under static and cyclic compressive loading. *J Eur Ceram Soc.* **21**, 1437-1440.

Calderon-Moreno J M. (2001). Stress induced domain switching of PZT in compression tests. *Materials Science and Engineering A.* **315**, 227-230.

Gu H, Moslehy Y, Sanders D, Song G and Mo Y L. (2010). Multi-functional smart aggregate-based structural health monitoring of circular reinforced concrete columns subjected to seismic excitations *Smart Materials and Structures.* **19**. 65026.

Gu H, Song G, Dhonde H, Mo Y L and Yan S. (2006). Concrete early-age strength monitoring using embedded piezoelectric transducers *Smart Materials and Structures.* **15**. 1837-1845.

IEEE (1988). IEEE Standard on Piezoelectricity.*ANSI-IEEE Std.* 176-1987.

Jayant S and Inderjit C. (2000). Fundamental Understanding of Piezoelectric Strain Sensors *J Intel Mat Syst Str*. **11**. 246-257.

Laskar A, Gu H, Mo Y L and Song G. (2009). Progressive collapse of a two-story reinforced concrete frame with embedded smart aggregates *Smart Materials and Structures*. **18**. 75001.

Li Z, Yang X and Li Z. (2006). Application of Cement-Based Piezoelectric Sensors for Monitoring Traffic Flows *Journal of Transportation Engineering*. **132**. 565-573.

Moslehy Y, Gu H, Belarbi A, Mo Y L and Song G. (2010). Smart aggregate based damage detection of circular RC columns under cyclic combined loading *Smart Materials and Structures*. **19**. 65021.

Song G, Gu H, Mo Y L, Hsu T, Dhonde H and Zhu R R H. (2005). Health monitoring of a concrete structure using piezoceramic materials. *SPIE*. **5765**. 108-119.

Song G, Olmi C and Gu H. (2007). An overheight vehicle-bridge collision monitoring system using piezoelectric transducers *Smart Materials and Structures*. **16**. 462-468.

Yan S, Sun W, Song G, Gu H, Huo L, Liu B and Zhang Y. (2009). Health monitoring of reinforced concrete shear walls using smart aggregates *Smart Materials and Structures.* **18**. 47001.

Yang W, Liu S, Ren W and Mukherjee B K. (2001). Effects of uniaxial stress on the piezoelectric, dielectric, and mechanical properties of lead zirconate titanate piezoceramics *Ferroelectrics* **262**. 207-212.

Yang X, Li Z, Ding Y and Li Z. (2005). Test on Sensor Effect of Cement Matrix Piezoelectric Composite *Transactions of Tianjin University* **11**. 133-136.

Yimnirun R, Laosiritaworn Y and Wongsaenmai S. (2006). Effect of uniaxial compressive pre-stress on ferroelectric properties of soft PZT ceramics *Journal of Physics D: Applied Physics.* **39**. 759-764.